

# ConceptPrism: Concept Disentanglement in Personalized Diffusion Models via Residual Token Optimization

Minseo Kim  
KAIST, South Korea  
alstj1571@kaist.ac.kr

Minchan Kwon  
KAIST, South Korea  
kmc0207@kaist.ac.kr

Dongyeun Lee  
KAIST, South Korea  
ledoye@kaist.ac.kr

Yunho Jeon<sup>†</sup>  
Hanbat National University, South Korea  
yhjeon@hanbat.ac.kr

Junmo Kim<sup>†</sup>  
KAIST, South Korea  
junmo.kim@kaist.ac.kr

## Abstract

Personalized text-to-image generation suffers from concept entanglement, where irrelevant residual information from reference images is captured, leading to a trade-off between concept fidelity and text alignment. Recent disentanglement approaches attempt to solve this utilizing manual guidance, such as linguistic cues or segmentation masks, which limits their applicability and fails to fully articulate the target concept. In this paper, we propose **ConceptPrism**, a novel framework that automatically disentangles the shared visual concept from image-specific residuals by comparing images within a set. Our method jointly optimizes a target token and image-wise residual tokens using two complementary objectives: a reconstruction loss to ensure fidelity, and a novel exclusion loss that compels residual tokens to discard the shared concept. This process allows the target token to capture the pure concept without direct supervision. Extensive experiments demonstrate that ConceptPrism effectively resolves concept entanglement, achieving a significantly improved trade-off between fidelity and alignment.

## 1. Introduction

The advent of text-to-image (T2I) diffusion models [18, 19, 22] has opened new frontiers in digital content creation. A key application attracting significant interest from both industry and the public is the creation of user-specific concepts like “my doll” or “my character” [3, 11, 20]. Given a handful of user-specific images, personalized generative models aim to implant a new concept into the model. The success of personalized generation is measured along two axes: *concept fidelity*, which preserves the visual essence of

<sup>†</sup>Joint corresponding authors.

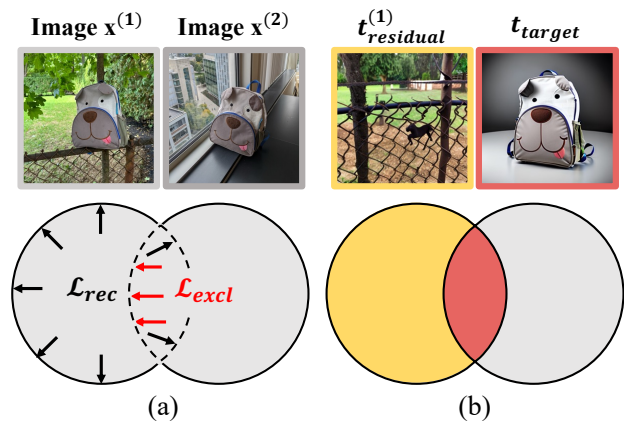


Figure 1. **Motivation of ConceptPrism.** The reconstruction loss ( $\mathcal{L}_{rec}$ ) promotes information acquisition from the given image, while the exclusion loss ( $\mathcal{L}_{excl}$ ) compels discarding the commonalities from the set. By jointly optimizing the target and residual tokens with dual losses, we disentangle the personalized visual concept from irrelevant details without explicit guidance.

the user’s concept, and *text alignment*, which ensures the generated image faithfully adheres to a given text prompt.

Existing personalization methods [3, 11, 20] typically fine-tune a pre-trained T2I diffusion model to map a target concept to a special token. However, this approach suffers from a critical limitation we term **concept entanglement**: the process inadvertently captures irrelevant residual information. As training progresses, the model may represent the target concept with higher detail, but also learns undesired attributes that conflict with new prompts. Concept entanglement leads to a trade-off between concept fidelity and text alignment, which degrades overall performance.

To tackle the concept entanglement problem, recent approaches [2, 5, 12, 27] provide context on “what to learn” by distributing image information across multiple tokens.

They attempt to separate information utilizing various manual guidance, such as linguistic cues [2, 5], segmentation masks [27], or auxiliary images [12]. DisenBooth [2] obtains an identity-preserved token for the class noun and an identity-irrelevant token by masking it. DisEnvisioner [5] trains a separate tokenizer to produce subject-essential and subject-irrelevant tokens leveraging class noun and the reference image. While effective, their reliance on manual guidance leads to incomplete disentanglement, as the guidance often fails to precisely articulate all visual details of the target concept. Furthermore, the cumbersome framework of injecting external guidance limits the types of concepts that can be applied.

To resolve this issue, we propose **ConceptPrism**, a novel framework that disentangles the commonalities and differences from a set of images into distinct tokens. Inspired by the human ability to identify shared concepts through simple comparison, our method captures the visual details of the target concept by comparing the images within the set, visualized in Figure 1. Specifically, we define a target token to capture the shared concept and a set of image-wise residual tokens to explicitly provide space for irrelevant, image-specific information. These tokens are jointly optimized via two complementary objectives. First, a **reconstruction loss** ensures that the combination of the target token and a residual token can faithfully represent each corresponding reference image. Second, an **exclusion loss**, applied only to the residual tokens, compels them to discard the common concept shared across the image set. This pressure creates an information vacuum within the residual tokens, which the target token must fill to satisfy the reconstruction objective, allowing it to capture the target concept without direct supervision.

Following token optimization, the disentangled tokens are injected as conditions to guide the fine-tuning of the T2I diffusion model. Their precise context on “what to learn” enables the model to focus only on the target concept, effectively reducing concept entanglement. Extensive experiments confirm that ConceptPrism achieves a significantly improved trade-off between text-alignment and concept fidelity, demonstrating that our method achieves accurate concept disentanglement. Requiring only a few images with a shared concept, our method is broadly applicable to diverse concept types, including objects, styles, and poses.

Our contributions are as follows:

- To the best of our knowledge, we are the first to disentangle the personalized concept through inter-image comparison in T2I diffusion models.
- We introduce an exclusion loss that enables the model to identify the shared concept without any external guidance, facilitating accurate disentanglement across a wide range of concept types.
- We propose ConceptPrism, a framework that resolves

concept entanglement and demonstrates superior generation ability, achieving a significantly improved trade-off between concept fidelity and text alignment in extensive experiments.

## 2. Preliminaries

### 2.1. Text-to-Image (T2I) Diffusion Models

Given a large-scale image dataset, diffusion models  $p_\theta$  approximate the true data distribution  $p_{data}$  via a tractable noise matching process [7, 25]. Specifically, Stable Diffusion [19], the model used in our study, employs a VAE [10] encoder  $\mathcal{E}(\cdot)$  to transform an input image  $\mathbf{x}$  into a low-dimensional latent representation  $\mathbf{z} = \mathcal{E}(\mathbf{x})$ . Given a noisy latent  $\mathbf{z}_t = \alpha_t \mathbf{z} + \sigma_t \epsilon$ , formulated with randomly sampled noise  $\epsilon \sim \mathcal{N}(0, I)$  and a timestep  $t \sim \mathcal{U}([0, 1])$ , the denoising model  $\epsilon_\theta$  is trained with the following objective:

$$\mathcal{L}_{DM} = \mathbb{E}_{\mathbf{z}, c, \epsilon, t} [w_t \|\epsilon - \epsilon_\theta(\mathbf{z}_t, t, \Gamma(c))\|_2^2], \quad (1)$$

where  $\Gamma(\cdot)$  denotes a text encoder like CLIP [17]. The terms  $\alpha_t$ ,  $\sigma_t$ , and  $w_t$  are hyperparameters defined by the noise schedule. The text condition  $c$  is injected into the cross-attention layers of the denoising model  $\epsilon_\theta$  to control the image generation process.

### 2.2. Personalized T2I Generative Models

Given a small set of user-specific images  $\{\mathbf{x}^{(i)}\}_{i=1}^N$ , there have been attempts [3, 11, 20] to implant a visual concept shared across images into a T2I diffusion model. The goal is to obtain a model that deeply understands and memorizes the personalized concept to generate diverse scenes.

We formally divide the abstract visual information in a single image  $\mathbf{x}^{(i)}$  into two parts:  $\{\mathcal{C}_{target}, \mathcal{C}_{residual}^{(i)}\}$ . The **target concept**  $\mathcal{C}_{target}$  represents the shared concept across all  $N$  images that the model is intended to learn. The image-wise **residual concept**  $\mathcal{C}_{residual}^{(i)}$  comprises the remaining image-specific elements after excluding  $\mathcal{C}_{target}$ .

Previous methods typically aim to map  $\mathcal{C}_{target}$  into a single target text token  $\mathbf{t}_{target}$ . This is achieved by optimizing either the token [3] or the model parameters [11, 20] to reconstruct the  $N$  images using the diffusion model loss, conditioned on  $\mathbf{t}_{target}$ . However, the reconstruction objective inevitably forces the token to also learn the residual concepts, causing  $\mathcal{C}_{residual}^{(i)}$  to become entangled with  $\mathbf{t}_{target}$ .

## 3. Our Approach: ConceptPrism

### 3.1. Image-wise Residual Tokens

To address the challenge of concept entanglement, we introduce **ConceptPrism**, a framework that automatically disentangles the target visual concept  $\mathcal{C}_{target}$  from image-specific

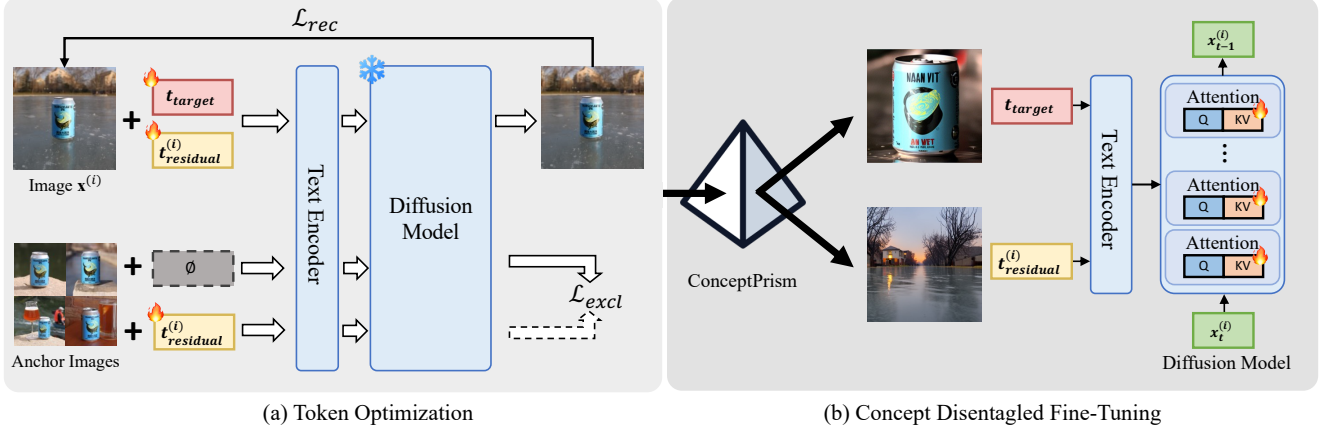


Figure 2. **Training Pipeline of ConceptPrism.** Our method comprises two stages: (a) In the Token Optimization, the target and image-wise residual tokens are jointly optimized via dual losses. The reconstruction loss ( $\mathcal{L}_{\text{rec}}$ ) guides the faithful reconstruction of the given image by conditioning on both tokens simultaneously. The exclusion loss ( $\mathcal{L}_{\text{excl}}$ ) forces the residual token to be uninformative of the shared target concept  $\mathcal{C}_{\text{target}}$  by matching the unconditional generation probability distribution. (b) In the Subsequent Fine-Tuning stage, the learned tokens initialize the model to focus only on the necessary concept, effectively resolving the trade-off caused by concept entanglement.

details. Our core strategy is to jointly optimize multiple text tokens: a single **target token**  $\mathbf{t}_{\text{target}}$  for  $\mathcal{C}_{\text{target}}$  and a set of **residual tokens**  $\{\mathbf{t}_{\text{residual}}^{(i)}\}_{i=1}^N$  for the image-specific concepts  $\{\mathcal{C}_{\text{residual}}^{(i)}\}_{i=1}^N$ .

When training on the  $i$ -th image  $\mathbf{x}^{(i)}$ , we provide a text condition  $c^{(i)}$  formatted as “ $\mathbf{t}_{\text{target}}$  with  $\mathbf{t}_{\text{residual}}^{(i)}$ ”. This ensures that the combination of two tokens can faithfully represent  $\mathbf{x}^{(i)}$ . Our reconstruction loss  $\mathcal{L}_{\text{rec}}$  is formulated as:

$$\mathcal{L}_{\text{rec}} = \sum_{i=1}^N \mathbb{E}_{\epsilon, t} \left[ w_t \left\| \epsilon - \epsilon_{\theta}(\mathbf{z}_t^{(i)}, t, \Gamma(c^{(i)})) \right\|_2^2 \right]. \quad (2)$$

### 3.2. Exclusion Loss for Concept Disentanglement

Alongside the reconstruction loss, we introduce an exclusion loss  $\mathcal{L}_{\text{excl}}$  to robustly disentangle concepts. Conditioning on both tokens using only  $\mathcal{L}_{\text{rec}}$  is not enough for proper disentanglement. The residual token  $\mathbf{t}_{\text{residual}}^{(i)}$  is trained exclusively on its corresponding image  $\mathbf{x}^{(i)}$ , which causes it to overfit by memorizing a single image. Such overfitting produce a trivial solution where  $\mathbf{t}_{\text{target}}$ , intended to represent all  $N$  images, converges to a state with no information.

To prevent the target concept from being absorbed into the residual tokens, our exclusion loss compels the residual tokens to discard  $\mathcal{C}_{\text{target}}$ . Its goal within the diffusion model  $p_{\theta}$  is to make the residual token  $\mathbf{t}_{\text{residual}}^{(i)}$  uninformative regarding the shared target concept  $\mathcal{C}_{\text{target}}$ . An “uninformative” state implies statistical independence: the given condition should not alter the probability distribution of generating the target concept. Therefore, the exclusion loss should guide  $\mathbf{t}_{\text{residual}}^{(i)}$  to avoid influencing the generative distribution for  $\mathcal{C}_{\text{target}}$ , compelling it to function as the null condition.

We formulate the objective using KL divergence, matching the generative distribution of  $\mathcal{C}_{\text{target}}$  under the null condition with the distribution conditioned on  $\mathbf{t}_{\text{residual}}^{(i)}$ . We substitute sampling from  $\mathcal{C}_{\text{target}}$  with using the given images  $\mathbf{x}^{(j)}$ , ( $j \neq i$ ). Since the diffusion model defines a generative process as a Markov chain of iterative reverse steps, our objective can be described as follows:

$$\min_{\{\mathbf{t}_{\text{residual}}^{(k)}\}_{k=1}^N} \mathbb{E}_{i, \mathbf{z}_t^{(j \neq i)}, t} \left[ D_{\text{KL}} \left( p_{\theta}(\mathbf{z}_{t-1}^{(j)} | \mathbf{z}_t^{(j)}, t, \emptyset) \parallel p_{\theta}(\mathbf{z}_{t-1}^{(j)} | \mathbf{z}_t^{(j)}, t, \Gamma(c_{\text{residual}}^{(i)})) \right) \right], \quad (3)$$

where  $c_{\text{residual}}^{(i)}$  is the text condition containing only the  $i$ -th residual token (e.g., “ $\mathbf{t}_{\text{residual}}^{(i)}$ ”). This objective can be simplified into the following tractable noise matching process, as derived in Appendix.

$$\mathcal{L}_{\text{excl}} = \mathbb{E}_{i, j \neq i, \epsilon, t} \left[ w_t \left\| \epsilon_{\theta}(\mathbf{z}_t^{(j)}, t, \Gamma(c_{\text{residual}}^{(i)})) - \epsilon_{\theta}(\mathbf{z}_t^{(j)}, t, \emptyset) \right\|_2^2 \right]. \quad (4)$$

Notably, the index of the image latent  $\mathbf{z}_t^{(j)}$  differs from that of the residual text condition  $c_{\text{residual}}^{(i)}$ , which constitutes the key idea behind this loss. Our final objective consists of dual losses, where hyperparameter  $\beta$  controls their relative importance:

$$\mathcal{L}_{\text{total}} = \mathcal{L}_{\text{rec}} + \beta \mathcal{L}_{\text{excl}}. \quad (5)$$

### 3.3. Better Initialization of Residual Tokens

Without careful residual token initialization, the concept disentanglement can be incomplete, with parts of the residual concept remaining entangled in  $\mathbf{t}_{\text{target}}$ . To ensure the

Method	CLIP-T $\uparrow$	DINO $\uparrow$	CLIP-I $\uparrow$	Training Time(s) $\downarrow$
Pretrained SD [19]	0.377 $\pm$ 0.024	0.167 $\pm$ 0.029	0.320 $\pm$ 0.030	-
DreamBooth-LoRA [20]	0.313 $\pm$ 0.030	<u>0.182</u> $\pm$ 0.030	0.331 $\pm$ 0.030	434.32 $\pm$ 75.50
Custom Diffusion [11]	<b>0.357</b> $\pm$ 0.023	0.178 $\pm$ 0.032	<u>0.341</u> $\pm$ 0.031	459.60 $\pm$ 59.64
DisenBooth [2]	<u>0.355</u> $\pm$ 0.027	0.170 $\pm$ 0.035	0.324 $\pm$ 0.033	928.63 $\pm$ 51.43
DisEnvisioner [5]	0.309 $\pm$ 0.023	0.171 $\pm$ 0.022	0.320 $\pm$ 0.024	-
ELITE [27]	0.293 $\pm$ 0.030	0.172 $\pm$ 0.031	<u>0.341</u> $\pm$ 0.032	-
ConceptPrism (Ours)	<b>0.357</b> $\pm$ 0.025	<b>0.210</b> $\pm$ 0.035	<b>0.353</b> $\pm$ 0.032	477.30 $\pm$ 91.29

Table 1. **Quantitative Evaluations on the DreamBench.** CLIP-T measures text alignment; DINO / CLIP-I assess concept fidelity. Training time to the best quality step was also measured (N/A for tuning-free approaches ELITE and DisEnvisioner). All experiments were repeated over 4 different seeds. Ours achieves the highest performance across all three metrics with negligible computational overhead.

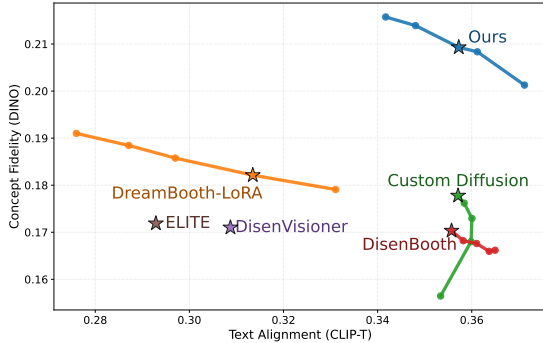


Figure 3. **Performance trade-off by training steps.** Our performance was measured at 40-step intervals, while other baselines were measured at 200-step intervals. Asterisk ( $\star$ ) denotes the best visual quality step for each method. Our curve demonstrates a superior trade-off compared to all baselines, highlighting its effective concept disentanglement.

residual token  $\mathbf{t}_{\text{residual}}^{(i)}$  comprehensively captures information other than  $\mathcal{C}_{\text{target}}$ , we initialize it to contain general information about the image  $\mathbf{x}^{(i)}$ . We feed a descriptive sentence (8-32 words) describing the whole scene of the given image into the CLIP encoder and use its mean embeddings as the starting point for the residual token.

Interestingly, our target token  $\mathbf{t}_{\text{target}}$  does not require initialization with any specific prior information. Unlike previous disentanglement strategies, which require at least a class noun for the target concept [2, 5, 12], our  $\mathbf{t}_{\text{target}}$  is initialized randomly and still successfully captures the intended concept. As training progresses, the residual tokens are forced to discard their commonality,  $\mathcal{C}_{\text{target}}$ , through inter-image comparison. This creates an information vacuum that the target token fills, allowing it to accurately acquire  $\mathcal{C}_{\text{target}}$  without direct supervision.

### 3.4. Concept Disentangled Fine-Tuning

The token optimization stage precisely isolates the intended concept into the target token. By encapsulating “what to learn” exactly, the target token enables diffusion models to focus on the necessary information. In the fine-tuning stage,

we train the model on reference images using  $\mathcal{L}_{\text{rec}}$ , providing the learned tokens as text conditions. The image-wise residual token is also provided alongside the target token, preventing unnecessary information from becoming associated with the target token. We insert LoRA [8] to modify only the attention layers of the diffusion model for parameter-efficient fine-tuning, as previous literatures [2, 15] have demonstrated that modifying only the attention layers retains sufficient expressiveness for personalization.

## 4. Experiments

### 4.1. Experimental Setup

**Datasets.** We evaluated our method on the DreamBench dataset [20], which includes 30 distinct personalized subjects, each with 4–6 reference images and 25 text prompts. For a robust quantitative evaluation, we generated 4 images for each {image, prompt} pair, resulting in a total of 3,000 images per method. We also used other open-source datasets for comprehensive qualitative analysis. [1, 9, 16].

**Implementation Details.** For training, we set a batch size of 1 with four gradient accumulation steps in 512x512 resolution. The learning rate was  $4e-4$  with the AdamW optimizer. We set the target and residual token lengths to 1 and 8, respectively, and the exclusion loss weight  $\beta$  to 0.05 by default. For inference, we adopted the DDIM [24] sampler with 25 steps and a classifier-free guidance [6] scale of 7.5. The token optimization stage ran for 200 steps, taking about 4 minutes on a single NVIDIA RTX 3090 GPU. The subsequent fine-tuning stage followed the same hyperparameters, achieving optimal quality after 120 steps. The performance was measured every 40 steps up to 200 steps of fine-tuning. Our pipeline was designed based on Stable Diffusion v2.1 [19], but it is applicable to other text-to-image diffusion model architectures.

**Baselines.** We compared our method against five baselines. DreamBooth [20] and Custom Diffusion [11] are



Figure 4. **Qualitative Results on various subjects.** Our method showed balanced performance, maintaining the visual details of the personalized subject while adhering to the text prompt. Other baselines tend to either copy input images (DreamBooth) or ignore concept representation to follow the prompt (Custom Diffusion, DisenBooth).

the most widely used fine-tuning methods for personalization. For lightweight training, the DreamBooth optimized only the attention layers of the diffusion model using LoRA [8], identical to our configuration in Section 3.4. ELITE [27], DisenBooth [2], and DisEnvisioner [5] are recent disentanglement-focused approaches. Among them, ELITE and DisEnvisioner are tuning-free approaches based on pre-trained encoders. All five baselines require a class noun for the target concept, and ELITE additionally requires a segmentation mask for the target object. We measured the performance of fine-tuning based approaches every 200 steps up to 1000 steps. DreamBooth, Custom Diffusion, and DisenBooth achieved their optimal visual quality at 400, 1000, and 1000 steps, respectively.

## 4.2. Quantitative Evaluations

**Evaluation Metrics.** We quantitatively measured performance from two aspects: text alignment and concept fidelity. For text alignment, we measured the cosine similarity between the text prompt and the generated images in the CLIP [17] feature space, denoted as CLIP-T [3, 20]. For concept fidelity, we measured the cosine similarity between reference and generated images in both DINOv2 (DINO) [14] and CLIP image spaces (CLIP-I). To ensure a precise evaluation, we applied binary masks on reference

images to isolate the target subject for fidelity scoring.

**Comparison with Baselines.** Table 1 reports the performance at the qualitatively optimal training steps for each method. The pre-trained SD [19] (before fine-tuning) serves as a baseline, representing an upper bound for CLIP-T and a lower bound for DINO and CLIP-I. Our method clearly demonstrates the highest performance in both text alignment (CLIP-T) and concept fidelity (DINO, CLIP-I). While Custom Diffusion and DisenBooth achieve competitive CLIP-T, their DINO scores are relatively low, showing little improvement over the baseline. DreamBooth achieves the second-best DINO score, indicating high concept fidelity. However, this comes at a significant cost to CLIP-T, suggesting overfitting to the reference images. In contrast, our method achieves a remarkable improvement in DINO score while maintaining a high CLIP-T, demonstrating that it effectively resolves the trade-off between the two metrics.

Figure 3 further illustrates our superior trade-off between text alignment (CLIP-T) and concept fidelity (DINO). While DreamBooth, DisenBooth, and our method all exchange text alignment for fidelity as training progresses, their slopes differ significantly. This highlights that our approach sacrifices the least text alignment for its fidelity gain. Furthermore, our high initial DINO scores (above 0.2)



Figure 5. **Qualitative Results on abstract styles.** Our method learns the abstract style beyond a single word class noun. DreamBooth generates similar scenes due to overfitting to the reference images. Other baselines fail to capture the given visual details, adhering only to the linguistic cues (e.g., “sunset,” “swirl”).

prove the token optimization stage acts as an effective initializer. Custom Diffusion maintains stable text alignment, but its fidelity plateaus after 1000 steps. Tuning-free methods DisEnvisioner and ELITE perform poorly on both metrics, showing the low precision of tuning-free techniques in concept representation.

**Training Time.** We also measured the training time for each method. While existing approaches train in a single diffusion model fine-tuning stage, our approach requires an additional token optimization process of approximately 200 steps. However, thanks to the better-initialized tokens, the number of model fine-tuning steps required to achieve sufficient concept fidelity is significantly reduced. For example, whereas DreamBooth achieves its optimal quality at 400 steps, our method shows improved performance with only 120 steps of training. As shown in Table 1, our method is approximately twice as fast as the existing disentanglement-focused approach, DisenBooth. Compared to DreamBooth and Custom Diffusion, it introduces only a minimal overhead considering the significant performance gain.

### 4.3. Qualitative Analysis

**Discrete Subject Personalization.** As visualized in Figure 4, our method faithfully adheres to the given text prompt while maintaining the high-fidelity visual details of the per-

sonalized subject. DreamBooth transforms background elements (e.g., red bricks, a jungle-style sofa) along with the subject and often reproduces compositions similar to the reference images. In contrast, our method transforms only the target subject in alignment with the prompt, implying our token separation strategy effectively prevents residual concept entanglement. Custom Diffusion and DisenBooth show high text alignment but suffer from low concept fidelity, tending to ignore the target subject as prompts become more complex. However, ours robustly preserves the detailed expression of the target concept even under challenging prompts. DisEnvisioner and ELITE, which generate from a single exemplar image without training, show limited understanding of the target concept.

**Abstract Style Personalization.** Our approach also excels at learning abstract styles, as shown in Figure 5. Custom Diffusion and DisEnvisioner adhere to the class noun, yet their generated styles bear little resemblance to the reference images. This indicates that their strategies, which rely on linguistic cues, fail to learn visual concepts that are difficult to describe verbally. In contrast, our method captures abstract styles beyond the scope of a single word by comparing across the image set. Notably, our method is the only one that comprehensively reflects the artistic details present in the given image set. DreamBooth reflects some aspects

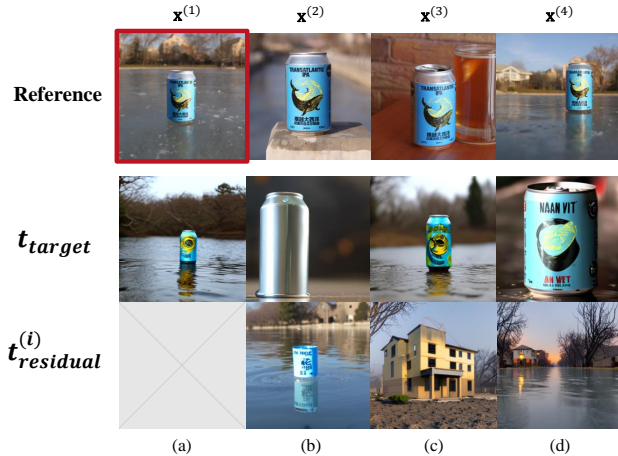


Figure 6. **Visualizations of Tokens after Token Optimization.** (a) Optimizing the target token alone. (b) Jointly optimizing target and residual tokens using the single objective  $\mathcal{L}_{rec}$ . (c) Optimizing with dual objectives by introducing  $\mathcal{L}_{excl}$ . (d) Initializing residual tokens with image descriptions.

of the given style but often struggles to generate creative scenes, frequently reproducing compositions similar to the reference images. ELITE cannot be applied here as it requires a binary mask for the target subject.

	CLIP-T $\uparrow$	DINO $\uparrow$
Target Token Optimization	0.345	0.197
+ Residual Tokens (Sec 3.1)	<b>0.358</b>	0.183
+ Exclusion Loss (Sec 3.2)	0.354	0.207
+ Better Initialization (Sec 3.3)	0.357	<b>0.210</b>

Table 2. **Ablation Studies on Token Optimization.** We measured performance by ablating each component of the token optimization stage. The introduction of residual tokens and the exclusion loss significantly improved CLIP-T and DINO, respectively, verifying their role in concept disentanglement.

$n$	0	1	2	4	8
CLIP-T	0.345	0.354	0.357	0.355	0.357
DINO	0.197	0.209	0.204	0.207	0.210

Table 3. **Performance by Residual Token Length.** The presence of residual tokens ( $n \geq 1$ ) creates a significant performance gap in both criteria, demonstrating their key role in resolving concept entanglement. The stable performance from  $n = 1$  to 8 indicates that our framework is robust to token length.

## 5. Ablation Studies

**Ablations on Token Optimization.** We investigate the impact of each component introduced in the token optimization process on concept disentanglement. Table 2 and

Figure 6 shows the results of the ablation experiment conducted under the same settings as the main experiments. (a) Optimizing the target token alone inevitably leads to concept entanglement. (b) When a residual token is added and optimized with  $\mathcal{L}_{rec}$ , the residual concept is effectively separated, leading to a significant improvement in text alignment. However, the target token fails to fully capture the common features across the given image set. (c) Adding  $\mathcal{L}_{excl}$  effectively guides the residual token to discard these common features. Consequently, the target token fully captures the target concept, leading to concept fidelity improvement. (d) Finally, initializing the residual token with image descriptions separates the concepts into the intended commonalities and differences, enhances both criteria.

**Influence of Residual Token Length.** Table 3 reports the quantitative evaluations as the residual token length  $n$  is varied. Both CLIP-T and DINO scores improve significantly when  $n \geq 1$ . This finding again demonstrates that the residual token is crucial for resolving the concept entanglement.

There is no significant performance difference for  $n$  between 1 and 8, implying that a capacity of one token is sufficient to capture the unnecessary residual concept. Furthermore, the performance remains stable even as  $n$  increases, despite the residual token having more capacity to store information. This stability proves that our exclusion loss prevents the residual token from absorbing the target concept.

**Visualizations of Residual Tokens.** To verify if our residual tokens truly learn image-wise residual information, we visualized the residual tokens after token optimization as shown in Figure 7. The learned residual token was used for T2I generation with the template ‘‘A photo of  $\mathbf{t}$ ’’. When the target concept is a discrete object, the residual token faithfully represents background details, camera angles, or lighting, excluding the object itself. When the target concept is a style, the residual token generates landscapes or objects with the target style removed. The ability to generate diverse images with the same semantics (e.g., offices with various layouts and arrangements) rather than simply copying the given images proves that our residual token actually learn image semantics instead of merely retaining its initial value.

## 6. Related Works

**Personalized T2I Generation.** Personalized text-to-image (T2I) generation aims to enable large-scale models to create novel images of a user-specific concept, learned from a small set of reference images. Existing methods can be broadly into two main paradigms based on their mechanisms: tuning-free and optimization-based approaches.

Tuning-free approaches, often referred to as encoder-based methods [5, 23, 27–29], excel at incorporating a concept for one-off generation tasks without fine-tuning the base model. To achieve high fidelity from a single shot,

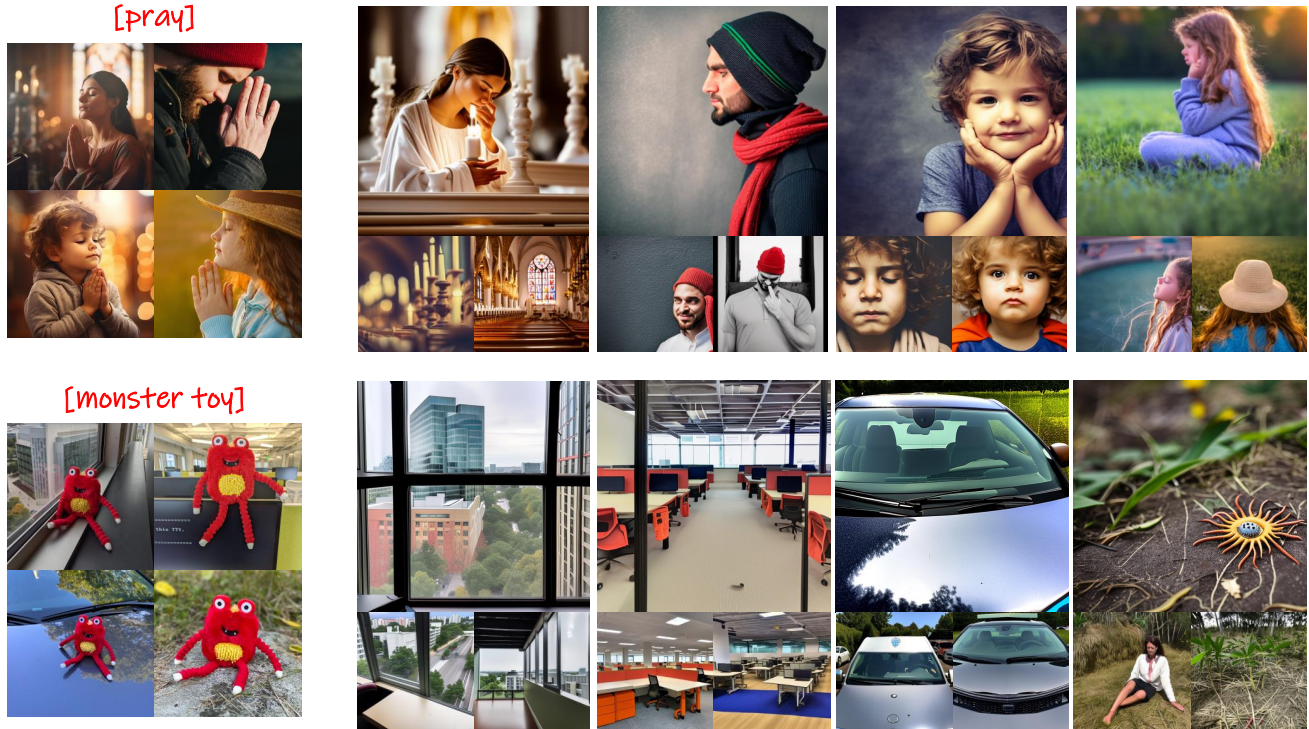


Figure 7. **Visualization of Learned Residual Tokens.** After the token optimization stage, an image-wise residual token can be solely conditioned to generate scene details without the target concept. We visualized the residual tokens learned from each reference image using three different seeds. The ability to generate diverse images of the same semantics (e.g., varied office layouts) rather than mere copies demonstrates that each token has learned an abstract residual concept.

they typically employ specialized encoders that have been pre-trained for specific domains, such as faces [21, 28], styles [13, 23], or human poses [29]. While effective, they struggle to persistently integrate the concept into the model or aggregate information from multiple references.

In contrast, optimization-based approaches [3, 11, 20] aim to create a durable model that persistently retains a user’s concept. This is particularly valuable for applications requiring high consistency across multiple generations. Textual Inversion [3] optimizes only a new token embedding while keeping the model frozen. DreamBooth [20] fine-tunes the entire diffusion model to better capture the subject’s details. Custom Diffusion [11] offers a more lightweight alternative by fine-tuning only a subset of cross-attention parameters. Subsequent works [4, 8, 26] have further improved efficiency by using parameter-efficient fine-tuning techniques. One popular variant adapts LoRA (Low-Rank Adaptation) [8], which injects small, trainable rank-decomposition matrices into the model’s layers, significantly reducing the number of trainable parameters.

**Disentanglement in Personalized Generation.** A central challenge in optimization-based personalization is concept entanglement, where the model memorizes irrelevant details along with the target concept. Existing studies to mitigate entanglement typically rely on various forms of explicit

guidance. ELITE [27] separates visual features from different layers of a CLIP image encoder, using its pre-defined feature hierarchy as guidance. DisenBooth [2] employs a learnable mask to remove regions corresponding to a class noun. Their residual tokens are obtained by applying this mask to the CLIP embeddings of the reference images. Dis-Envisioner [5] trains a separate tokenizer, disentangling the image into an embedding corresponding to the class noun and a residual embedding. Similarly, Lego [12] guides the separation by requiring an additional set of images where the concept is absent. This shared reliance on external guidance limits their applicability to abstract concepts that are difficult to describe or segment and can introduce complex dependencies into the pipeline. In contrast, our work proposes a more flexible and self-contained disentanglement strategy that operates without guidance.

## 7. Conclusions

In this paper, we introduced ConceptPrism, a novel framework designed to resolve concept entanglement in personalized text-to-image generation. Unlike existing approaches that rely on manual guidance, our method automatically disentangles the shared visual concept from image-specific residuals through inter-image comparison. By jointly optimizing target and residual tokens with complementary reconstruction and exclusion objectives, the target token cap-

tures the detailed visual concept without explicit supervision. Extensive experiments demonstrate that ConceptPrism significantly improves the trade-off between concept fidelity and text alignment, establishing a robust and broadly applicable solution for diverse personalization tasks.

## References

- [1] Freepik. <https://www.freepik.com/>, 2025. 4, 3
- [2] Hong Chen, Yipeng Zhang, Simin Wu, Xin Wang, Xuguang Duan, Yuwei Zhou, and Wenwu Zhu. Disenbooth: Identity-preserving disentangled tuning for subject-driven text-to-image generation. *arXiv preprint arXiv:2305.03374*, 2023. 1, 2, 4, 5, 8
- [3] Rinon Gal, Yuval Alaluf, Yuval Atzmon, Or Patashnik, Amit Haim Bermano, Gal Chechik, and Daniel Cohen-or. An image is worth one word: Personalizing text-to-image generation using textual inversion. In *The Eleventh International Conference on Learning Representations*, 2022. 1, 2, 5, 8
- [4] Ligong Han, Yinxiao Li, Han Zhang, Peyman Milanfar, Dimitris Metaxas, and Feng Yang. Svdiff: Compact parameter space for diffusion fine-tuning. In *Proceedings of the IEEE/CVF International Conference on Computer Vision*, pages 7323–7334, 2023. 8
- [5] Jing He, LI Haodong, Guibao Shen, CAI Yingjie, Weichao Qiu, Ying-Cong Chen, et al. Disenvisioner: Disentangled and enriched visual prompt for customized image generation. In *The Thirteenth International Conference on Learning Representations*, 2024. 1, 2, 4, 5, 7, 8
- [6] Jonathan Ho and Tim Salimans. Classifier-free diffusion guidance. In *NeurIPS 2021 Workshop on Deep Generative Models and Downstream Applications*, 2022. 4
- [7] Jonathan Ho, Ajay Jain, and Pieter Abbeel. Denoising diffusion probabilistic models. *Advances in neural information processing systems*, 33:6840–6851, 2020. 2, 1
- [8] Edward J Hu, Yelong Shen, Phillip Wallis, Zeyuan Allen-Zhu, Yuanzhi Li, Shean Wang, Lu Wang, Weizhu Chen, et al. Lora: Low-rank adaptation of large language models. *ICLR*, 1(2):3, 2022. 4, 5, 8
- [9] Siteng Huang, Biao Gong, Yutong Feng, Xi Chen, Yuqian Fu, Yu Liu, and Donglin Wang. Learning disentangled identifiers for action-customized text-to-image generation. In *Proceedings of the IEEE/CVF Conference on Computer Vision and Pattern Recognition*, pages 7797–7806, 2024. 4, 3
- [10] Diederik P Kingma, Max Welling, et al. Auto-encoding variational bayes, 2013. 2
- [11] Nupur Kumari, Bingliang Zhang, Richard Zhang, Eli Shechtman, and Jun-Yan Zhu. Multi-concept customization of text-to-image diffusion. In *Proceedings of the IEEE/CVF conference on computer vision and pattern recognition*, pages 1931–1941, 2023. 1, 2, 4, 8, 3
- [12] Saman Motamed, Danda Pani Paudel, and Luc Van Gool. Lego: Learning to disentangle and invert personalized concepts beyond object appearance in text-to-image diffusion models. In *European Conference on Computer Vision*, pages 116–133. Springer, 2024. 1, 2, 4, 8
- [13] Chong Mou, Xintao Wang, Liangbin Xie, Yanze Wu, Jian Zhang, Zhongang Qi, and Ying Shan. T2i-adapter: Learning adapters to dig out more controllable ability for text-to-image diffusion models. In *Proceedings of the AAAI conference on artificial intelligence*, pages 4296–4304, 2024. 8
- [14] Maxime Oquab, Timothée Darcet, Théo Moutakanni, Huy Vo, Marc Szafraniec, Vasil Khalidov, Pierre Fernandez, Daniel Haziza, Francisco Massa, Alaaeldin El-Nouby, et al. Dinov2: Learning robust visual features without supervision. *arXiv preprint arXiv:2304.07193*, 2023. 5
- [15] Sunghyun Park, Seokeon Choi, Hyoungwoo Park, and Sung-rack Yun. Steering guidance for personalized text-to-image diffusion models. In *Proceedings of the IEEE/CVF International Conference on Computer Vision*, pages 15907–15916, 2025. 4
- [16] Yuang Peng, Yuxin Cui, Haomiao Tang, Zekun Qi, Runpei Dong, Jing Bai, Chunrui Han, Zheng Ge, Xiangyu Zhang, and Shu-Tao Xia. Dreambench++: A human-aligned benchmark for personalized image generation. *arXiv preprint arXiv:2406.16855*, 2024. 4
- [17] Alec Radford, Jong Wook Kim, Chris Hallacy, Aditya Ramesh, Gabriel Goh, Sandhini Agarwal, Girish Sastry, Amanda Askell, Pamela Mishkin, Jack Clark, et al. Learning transferable visual models from natural language supervision. In *International conference on machine learning*, pages 8748–8763. PmLR, 2021. 2, 5
- [18] Aditya Ramesh, Prafulla Dhariwal, Alex Nichol, Casey Chu, and Mark Chen. Hierarchical text-conditional image generation with clip latents. *arXiv preprint arXiv:2204.06125*, 1(2):3, 2022. 1
- [19] Robin Rombach, Andreas Blattmann, Dominik Lorenz, Patrick Esser, and Björn Ommer. High-resolution image synthesis with latent diffusion models. In *Proceedings of the IEEE/CVF conference on computer vision and pattern recognition*, pages 10684–10695, 2022. 1, 2, 4, 5
- [20] Nataniel Ruiz, Yuanzhen Li, Varun Jampani, Yael Pritch, Michael Rubinstein, and Kfir Aberman. Dreambooth: Fine tuning text-to-image diffusion models for subject-driven generation. In *Proceedings of the IEEE/CVF conference on computer vision and pattern recognition*, pages 22500–22510, 2023. 1, 2, 4, 5, 8
- [21] Nataniel Ruiz, Yuanzhen Li, Varun Jampani, Wei Wei, Tingbo Hou, Yael Pritch, Neal Wadhwa, Michael Rubinstein, and Kfir Aberman. Hyperdreambooth: Hypernetworks for fast personalization of text-to-image models. In *Proceedings of the IEEE/CVF conference on computer vision and pattern recognition*, pages 6527–6536, 2024. 8
- [22] Chitwan Saharia, William Chan, Saurabh Saxena, Lala Li, Jay Whang, Emily L Denton, Kamyar Ghasemipour, Raphael Gontijo Lopes, Burcu Karagol Ayan, Tim Salimans, et al. Photorealistic text-to-image diffusion models with deep language understanding. *Advances in neural information processing systems*, 35:36479–36494, 2022. 1
- [23] Jing Shi, Wei Xiong, Zhe Lin, and Hyun Joon Jung. Instantbooth: Personalized text-to-image generation without test-time finetuning. In *Proceedings of the IEEE/CVF conference on computer vision and pattern recognition*, pages 8543–8552, 2024. 7, 8

- [24] Jiaming Song, Chenlin Meng, and Stefano Ermon. Denoising diffusion implicit models. *arXiv preprint arXiv:2010.02502*, 2020. [4](#)
- [25] Yang Song, Jascha Sohl-Dickstein, Diederik P Kingma, Abhishek Kumar, Stefano Ermon, and Ben Poole. Score-based generative modeling through stochastic differential equations. *arXiv preprint arXiv:2011.13456*, 2020. [2](#)
- [26] Yoad Tewel, Rinon Gal, Gal Chechik, and Yuval Atzmon. Key-locked rank one editing for text-to-image personalization. In *ACM SIGGRAPH 2023 conference proceedings*, pages 1–11, 2023. [8](#)
- [27] Yuxiang Wei, Yabo Zhang, Zhilong Ji, Jinfeng Bai, Lei Zhang, and Wangmeng Zuo. Elite: Encoding visual concepts into textual embeddings for customized text-to-image generation. In *Proceedings of the IEEE/CVF International Conference on Computer Vision*, pages 15943–15953, 2023. [1](#), [2](#), [4](#), [5](#), [7](#), [8](#)
- [28] Guangxuan Xiao, Tianwei Yin, William T Freeman, Frédo Durand, and Song Han. Fastcomposer: Tuning-free multi-subject image generation with localized attention. *International Journal of Computer Vision*, pages 1–20, 2024. [8](#)
- [29] Hu Ye, Jun Zhang, Sibor Liu, Xiao Han, and Wei Yang. Ip-adapter: Text compatible image prompt adapter for text-to-image diffusion models. *arXiv preprint arXiv:2308.06721*, 2023. [7](#), [8](#)

# ConceptPrism: Concept Disentanglement in Personalized Diffusion Models via Residual Token Optimization

## Supplementary Material

### 8. Derivation of Equation 4

The objective of our exclusion loss is to ensure that the residual token  $\mathbf{t}_{\text{residual}}^{(i)}$  remains uninformative regarding the target concept when reconstructing other images  $\mathbf{x}^{(j)}$  where  $j \neq i$ . As explained in Section 3.2, this is achieved by minimizing the KL divergence between the distribution conditioned on the residual token and the unconditional distribution:

$$\mathcal{L}_{\text{KL}} = \mathbb{E}_{i, \mathbf{z}_t^{(j \neq i)}, t} \left[ D_{\text{KL}} \left( p_{\theta}(\mathbf{z}_{t-1}^{(j)} | \mathbf{z}_t^{(j)}, t, \emptyset) \parallel p_{\theta}(\mathbf{z}_{t-1}^{(j)} | \mathbf{z}_t^{(j)}, t, \Gamma(c_{\text{residual}}^{(i)})) \right) \right]. \quad (6)$$

In diffusion models [19], the reverse process  $p_{\theta}(\mathbf{z}_{t-1} | \mathbf{z}_t, t, \mathbf{c})$  is parameterized as a Gaussian distribution  $\mathcal{N}(\mathbf{z}_{t-1}; \boldsymbol{\mu}_{\theta}(\mathbf{z}_t, t, \mathbf{c}), \boldsymbol{\Sigma}_{\theta}(\mathbf{z}_t, t))$ . Following standard practice [7], we fix the covariance matrix  $\boldsymbol{\Sigma}_{\theta}$  to a time-dependent constant  $\beta_t \mathbf{I}$ . The cumulative signal scale  $\bar{\alpha}_t$  is defined as  $\bar{\alpha}_t = \prod_{s=1}^t (1 - \beta_s)$  following DDPM notation [7], based on the noise schedule  $\beta_t$ . Under the assumption of equal covariance, the KL divergence between two Gaussians is proportional to the squared Euclidean distance between their means:

$$D_{\text{KL}}(\mathcal{N}(\boldsymbol{\mu}_1, \boldsymbol{\Sigma}) \parallel \mathcal{N}(\boldsymbol{\mu}_2, \boldsymbol{\Sigma})) \propto \|\boldsymbol{\mu}_1 - \boldsymbol{\mu}_2\|_2^2. \quad (7)$$

Thus, minimizing  $\mathcal{L}_{\text{KL}}$  is equivalent to minimizing the distance between the predicted means given the null condition  $\emptyset$  and the residual condition  $c_{\text{residual}}^{(i)}$ . The mean  $\boldsymbol{\mu}_{\theta}$  is related to the noise prediction  $\boldsymbol{\epsilon}_{\theta}$  by:

$$\boldsymbol{\mu}_{\theta}(\mathbf{z}_t, t, \mathbf{c}) = \frac{1}{\sqrt{1 - \beta_t}} \left( \mathbf{z}_t - \frac{\beta_t}{\sqrt{1 - \bar{\alpha}_t}} \boldsymbol{\epsilon}_{\theta}(\mathbf{z}_t, t, \mathbf{c}) \right). \quad (8)$$

Substituting this into the distance metric, the terms involving  $\mathbf{z}_t$  cancel out, simplifying the objective to the difference between noise predictions:

$$\begin{aligned} & \left\| \boldsymbol{\mu}_{\theta}(\mathbf{z}_t^{(j)}, t, \emptyset) - \boldsymbol{\mu}_{\theta}(\mathbf{z}_t^{(j)}, t, \Gamma(c_{\text{residual}}^{(i)})) \right\|_2^2 \\ &= \left\| \frac{1}{\sqrt{1 - \beta_t}} \left( \mathbf{z}_t^{(j)} - \frac{\beta_t}{\sqrt{1 - \bar{\alpha}_t}} \boldsymbol{\epsilon}_{\theta}(\mathbf{z}_t^{(j)}, t, \emptyset) \right) \right. \\ & \quad \left. - \frac{1}{\sqrt{1 - \beta_t}} \left( \mathbf{z}_t^{(j)} - \frac{\beta_t}{\sqrt{1 - \bar{\alpha}_t}} \boldsymbol{\epsilon}_{\theta}(\mathbf{z}_t^{(j)}, t, \Gamma(c_{\text{residual}}^{(i)})) \right) \right\|_2^2 \\ &= \frac{\beta_t^2}{(1 - \bar{\alpha}_t)(1 - \beta_t)} \left\| \boldsymbol{\epsilon}_{\theta}(\mathbf{z}_t^{(j)}, t, \Gamma(c_{\text{residual}}^{(i)})) - \boldsymbol{\epsilon}_{\theta}(\mathbf{z}_t^{(j)}, t, \emptyset) \right\|_2^2. \end{aligned} \quad (9)$$

By absorbing the scalar coefficients  $\frac{\beta_t^2}{(1 - \bar{\alpha}_t)(1 - \beta_t)}$  into the weighting term  $w_t$  and summing over all valid pairs  $(i, j)$  where  $j \neq i$ , we arrive at the final exclusion loss presented in Equation 4.

### 9. More Experimental Details

**Algorithms.** The exact implementation of ConceptPrism are summarized in Algorithm 1 and Algorithm 2. Algorithm 1 outlines the token optimization stage in Section 3.1 to 3.3, where the target and residual tokens are jointly optimized. Algorithm 2 describes the subsequent concept disentangled fine-tuning stage in Section 3.4. For computational efficiency, we approximate the exclusion loss  $\mathcal{L}_{\text{excl}}$  during the token optimization. Instead of utilizing the entire set of  $N - 1$  negative samples, we randomly sample a subset of 3 indices  $\mathcal{J} \subset \{k \mid k \neq i\}$  at each iteration.

**Image Captions on Section 3.3.** We employed a Vision Language Model (VLM), specifically Gemini 2.5 Flash, to generate descriptive captions for each reference image. These captions serve as the initialization for residual tokens (Section 3.3). The specific prompt used is provided below. Note that this initialization captures the overall scene, ensuring the initial tokens are not biased toward either the target concept or specific residuals.

#### Prompt for Scene Description

You are an AI that describes visual scenes in detail. Your mission is to describe a given image using 8-32 words of text.

#### Instructions

1. **Purpose of Description:** Describe the image in sufficient detail that the original scene can be visually **reconstructed** based **solely on the text description**.
2. **Elements to Describe:** You must include not only the main **subject** but also the core visual elements that constitute the scene, such as its key **attributes, background, composition, lighting, and style**.
3. All descriptions must be written in English and be between 8 and 32 words.

---

**Algorithm 1** Token Optimization

---

**Require:** Reference images  $\mathcal{X} = \{\mathbf{x}^{(i)}\}_{i=1}^N$ , Pre-trained Model  $\epsilon_\theta$ , Exclusion weight  $\beta$ , Total timesteps  $T$

**Ensure:** Optimized tokens  $\mathbf{t}_{\text{target}}, \{\mathbf{t}_{\text{residual}}^{(i)}\}_{i=1}^N$

- 1: Initialize  $\mathbf{t}_{\text{target}}$  randomly
- 2: Initialize  $\{\mathbf{t}_{\text{residual}}^{(i)}\}_{i=1}^N$  with caption embeddings of  $\{\mathbf{x}^{(i)}\}_{i=1}^N$
- 3: **while** not converged **do**
- 4:   Sample  $i \sim \mathcal{U}(1, N)$  and  $\mathbf{x}^{(i)} \sim \mathcal{X}$
- 5:   Sample  $\epsilon \sim \mathcal{N}(\mathbf{0}, \mathbf{I}), t \sim \mathcal{U}(\{1, \dots, T\})$
- 6:   // Compute Reconstruction Loss
- 7:    $c^{(i)} \leftarrow$  “ $\mathbf{t}_{\text{target}}$  with  $\mathbf{t}_{\text{residual}}^{(i)}$ ”
- 8:    $\mathcal{L}_{\text{rec}} \leftarrow \|\epsilon - \epsilon_\theta(\mathbf{z}_t^{(i)}, t, \Gamma(c^{(i)}))\|_2^2$
- 9:   // Compute Exclusion Loss
- 10:   Sample  $\mathcal{J} \subset \{k \mid k \neq i\}$  s.t.  $|\mathcal{J}| = 3$
- 11:    $\mathcal{L}_{\text{excl}} \leftarrow 0$
- 12:   **for**  $j \in \mathcal{J}$  **do**
- 13:      $\mathcal{L}_{\text{excl}} \leftarrow \mathcal{L}_{\text{excl}} + \|\epsilon_\theta(\mathbf{z}_t^{(j)}, t, \Gamma(\mathbf{t}_{\text{residual}}^{(i)})) - \epsilon_\theta(\mathbf{z}_t^{(j)}, t, \emptyset)\|_2^2$
- 14:   **end for**
- 15:   Update  $\mathbf{t}_{\text{target}}, \mathbf{t}_{\text{residual}}^{(i)}$  via  $\nabla(\mathcal{L}_{\text{rec}} + \beta\mathcal{L}_{\text{excl}})$
- 16: **end while**

---

---

**Algorithm 2** Concept Disentangled Fine-Tuning

---

**Require:** Reference images  $\mathcal{X} = \{\mathbf{x}^{(i)}\}_{i=1}^N$ , Optimized tokens  $\mathbf{t}_{\text{target}}, \{\mathbf{t}_{\text{residual}}^{(i)}\}_{i=1}^N$ , Model  $\epsilon_\theta$ , Total timesteps  $T$

**Ensure:** Personalized Model  $\epsilon_{\theta^*}$

- 1: Fix  $\mathbf{t}_{\text{target}}$  and  $\{\mathbf{t}_{\text{residual}}^{(i)}\}_{i=1}^N$
- 2: Inject LoRA parameters  $\theta_{\text{loRa}}$  into attention layers of  $\epsilon_\theta$
- 3: **while** not converged **do**
- 4:   Sample batch  $(i, \mathbf{x}^{(i)})$  from  $\mathcal{X}$
- 5:   Sample  $\epsilon \sim \mathcal{N}(\mathbf{0}, \mathbf{I}), t \sim \mathcal{U}(\{1, \dots, T\})$
- 6:   // Fine-tune with disentangled tokens
- 7:    $c \leftarrow$  “ $\mathbf{t}_{\text{target}}$  with  $\mathbf{t}_{\text{residual}}^{(i)}$ ”
- 8:    $\mathcal{L}_{\text{ft}} \leftarrow \|\epsilon - \epsilon_\theta(\mathbf{z}_t^{(i)}, t, \Gamma(c))\|_2^2$
- 9:   Update  $\theta_{\text{loRa}}$  via  $\nabla \mathcal{L}_{\text{ft}}$
- 10: **end while**

---

## 10. Ablation Studies

**Impact of Target Token Length.** We investigated the impact of the target token length ( $n$ ) on performance. A longer token sequence theoretically provides greater capacity to encode visual information. We evaluated lengths of  $n \in \{1, 2, 4, 8\}$  as summarized in Table 4. The results indicate that  $n = 1$  yields the optimal balance. Increasing  $n$  marginally improves Concept Fidelity (DINO) but significantly degrades Text Alignment (CLIP-T).

This trade-off suggests that a high-capacity target token captures excessive details and leads to conflicts with the

text prompt. This phenomenon may stem from the transformer, which struggles to handle extended contexts, or the concept entanglement of the target token. Specifically, an over-parameterized target token risks memorizing the entire reference images including residuals, regardless of the exclusion loss applied to residual tokens. While introducing a mechanism to minimize the information overlap between target and residual tokens remains a promising direction for future work, our empirical results confirm that a single token ( $n = 1$ ) provides sufficient capacity for effectively capturing most concepts.

$n$	1	2	4	8
CLIP-T	0.357	0.352	0.339	0.325
DINO	0.210	0.207	0.212	0.220

Table 4. **Impact of Target Token Length.**  $n$  denotes the length of the target token. We adopted  $n = 1$  for our main experiments.

**Impact of Exclusion Loss Weight.** We analyzed the impact of the exclusion loss weight  $\beta$  on model performance. (Table 5). The results show that introducing  $\mathcal{L}_{\text{excl}}$  significantly improves Concept Fidelity (DINO) compared to the baseline without exclusion loss ( $\beta = 0$ ). This confirms that our exclusion objective effectively prevents residual tokens from absorbing the target concept.

However, an excessively large  $\beta$  leads to a degradation in Text Alignment (CLIP-T). A strong penalty forces residual tokens to discard necessary image-specific details and converge towards a null condition. Consequently, the target token inadvertently captures this residual information to minimize the reconstruction loss. Our experiments suggest that  $\beta = 0.05$  yields the optimal trade-off.

$\beta$	0	0.01	0.05	0.1	0.5
CLIP-T	0.358	0.356	0.354	0.346	0.347
DINO	0.183	0.198	0.207	0.209	0.206

Table 5. **Impact of Exclusion Loss Weight.** We adopted the exclusion loss weight  $\beta = 0.05$  for our main experiments.

## 11. Additional Experiments

**VLM Evaluations.** Standard quantitative metrics often diverge from human perception. To assess practical performance, we conducted an evaluation using a VLM. Specifically, we employed GPT-4o on 24 random concept-prompt pairs from DreamBench. The VLM evaluated images based on three criteria: (1) *Concept Fidelity*, (2) *Text Alignment*, and (3) *Overall Preference*, providing a binary decision

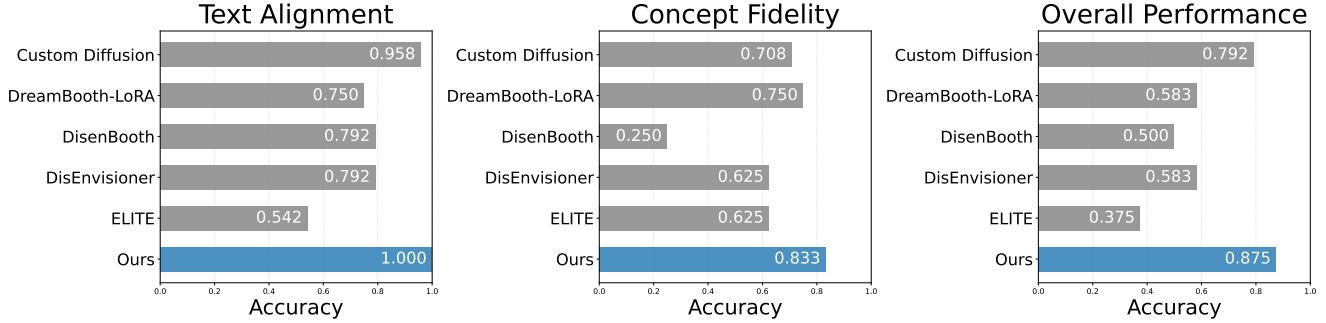


Figure 8. **VLM Evaluations.** We prompted GPT-4o to assess generated images on three criteria: Concept Fidelity, Text Alignment, and Overall Preference. The charts display the satisfaction rates for each method. Our method consistently outperforms baselines across all metrics, validating the effectiveness of our disentanglement framework.

(satisfy/unsatisfy) for each. Figure 8 summarizes the satisfaction rates. Our method consistently achieved the highest scores across all criteria, demonstrating the effectiveness of our disentanglement framework.

The specific prompts used for the evaluation are detailed below.

### Evaluation Prompts

- **Text Alignment:**

*“You are an impartial and unambiguous judge who must evaluate the quality of the given picture. You must assign either 1 (satisfies the condition) or 0 (does not). The condition is: ‘Does the picture reflect the following text prompt? - Text Prompt: {text\_prompt}’ Please output a single digit (1 or 0).”*

- **Concept Fidelity:**

*“You are an impartial and unambiguous judge who must evaluate the quality of the given picture. You must assign either 1 (satisfies the condition) or 0 (does not). The condition is: ‘Does the picture faithfully follow the visual details of the source images?’ Please output a single digit (1 or 0).”*

- **Overall Preference:**

*“You are an impartial and unambiguous judge who must evaluate the quality of the given picture. You must assign either 1 (satisfies the condition) or 0 (does not). The condition is: ‘Considering both the text prompt and the source images, does the given picture follow both the text prompt and source visual details?’ Please output a single digit (1 or 0).”*

**Application on Other Backbone Models.** Our framework fundamentally operates through text token disentanglement, making it applicable to any text-to-image model featuring a text encoder regardless of the backbone architecture (e.g., UNet or DiT). This architectural agnosticism highlights the scalability of our method. Figure 9 presents the experimental results on the black-forest-labs/FLUX.1-dev model, which employs a Diffusion Transformer (DiT) architecture, distinct from the UNet backbone of SDv2.1 used in our main experiments. For memory-efficient training on a single NVIDIA RTX 3090 GPU, we applied 4-bit quantization to the transformer and set the compute dtype of all modules to bfloat16. We utilized the 8-bit AdamW optimizer and trained at a resolution of  $512 \times 512$ .

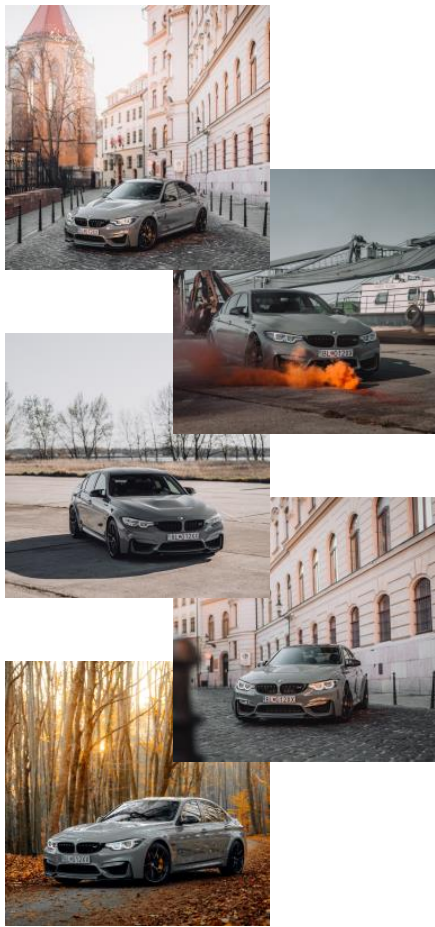
**More Flexible Modifications on Learned Concepts.**

Most personalization methods bind the learned concept to a specific coarse class noun (e.g., “dog” or “book”) during the optimization process. In contrast, ConceptPrism extracts the target concept without such semantic priors. This independence allows for fundamental semantic shifts during generation. As shown in Figure 10, our model can transfer learned visual attributes onto entirely different object categories (e.g., transforming a specific book design into a box). This capability demonstrates that our token captures intrinsic visual structures rather than being tied to a linguistic class. We conducted these experiments using the Custom-Concept101 [11] dataset.

**More Results on Abstract Concepts.**

We present further examples demonstrating our method’s capability to capture abstract concepts that are difficult to describe verbally. We utilized datasets from Freepik [1] and ActionBench [9] for these experiments. The results in Figure 11 demonstrate that our learned token effectively captures abstract semantics, color palettes, and artistic styles from the given images.

## References



## Generated Images



A [v] in the desert



A golden [v]



A top view of [v]

Figure 9. **Application on FLUX.1.** Since our framework operates on the text embedding space, it is agnostic to the backbone architecture of the diffusion model. We demonstrate this broad applicability by successfully generating personalized images using the FLUX.1-dev model.

## References



## Generated Images



Book  $\Rightarrow$  Box



Cat  $\Rightarrow$  Wolf



Dog  $\Rightarrow$  Doll



Purse  $\Rightarrow$  Bag

Figure 10. **Flexible modifications on learned concepts.** Since our method learns without class noun guidance, the learned token can be flexibly applied to different subject classes. To generate these images, we used prompts specifying a new subject class, such as “A photo of [target] box” or “A photo of [target] wolf”.

## References



## Generated Images



"A cat doing [V]"



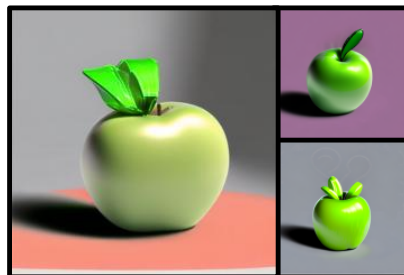
"An old man on the mountain doing [V]"



"Doctors of [V] style"



"A party of [V] style"



"A green apple of [V] style"



"A tree of [V] style"

Figure 11. **Additional results on abstract concepts.** Our method effectively disentangles and learns abstract concepts from various datasets, including styles and actions.